Microelectronic Engineering 191 (2018) 38–41

Contents lists available at ScienceDirect

Microelectronic Engineering

journal homepage: www.elsevier.com/locate/mee

Accelerated publication

High resolution polymer coated strain sensors for in-liquid operation

Francesca Sorba, Cristina Martin-Olmos *

Centre Suisse d'Electronique et de Microelectronique CSEM SA, CH-2002 Neuchâtel, Switzerland

ARTICLE INFO

Article history:
Received 23 January 2018
Accepted 24 January 2018
Available online 31 January 2018

Keywords:
Strain sensor
Polymer MEMS
Metallic gauges

ABSTRACT

Metallic strain gauges are well studied structures for their use in force sensing. Their fabrication is rather simple, easily compatible with many techniques are broadly scalable in both quantity and resolution. Here we present a fabrication process for high resolution strain sensors (down to the nN) that can also be operated in liquid, i.e. for life sciences applications. This fabrication method offers a very high yield and opens new possibilities for bioengineering, as for example single cell studies.

1. Introduction

Polymer-based micromechanical systems (MEMS) have been increasingly used in biomedical applications [1,2]. They offer several advantages over conventional fabrication methods such as lower costs, lightness, transparency, flexibility and biocompatibility [3]. This is why, several types of MEMS like microfluidic devices [4], pressure sensors [5], implantable devices [6], tactile sensors [7] and temperature sensors [8] have already a polymer-based version. Of particular interest for cell studies are high sensitivity force sensors, which are typically addressed with the optical processing of bending structures like arrays of narrow pillars [9]. However, this high force sensitivity cannot be achieved for a large measurement bandwidth. In order to achieve larger bandwidth, it is more advantageous to move into an electrical read-out.

Microscale strain sensors are of particular interest in MEMS because of their ability to measure force, acceleration, pressure or sound and their broad applicability in robotics, space based systems, sports and therapeutics. They provide an integrated solution for electrical read-out, allowing simple data acquisition and processing in addition to the mentioned larger measurement bandwidth compared to optical techniques [10]. MEMS force sensors with electrical detection have long been proposed and demonstrated via piezoresistive detection [11,12] and metallic strain gauges [13] among others.

This latter concept has been presented in the past within polymer-based MEMS [6,14,15]. The choice of the polymer structural material is quite critical to determine the sensitivity of the final measurement. Among the most versatile materials for fabricating highly flexible strain gauges is polydimethylsiloxane (PDMS) due to its simple fabrication, biocompatibility and low Young's modulus. One method to implement strain gauges on PDMS is by directly depositing metal on top of a PDMS layer. This method has successfully been used to fabricate implantable strain sensors to assess bone morphology [6] or for neuroprosthetic applications [15]. However, the presence of thin metallic layers affects strongly the overall stiffness of the structure. When high flexibility is needed, it is more convenient to replace metal for fillers such as conductive carbon fibers [16], carbon nanotubes [17] and graphene [18]. Overall, the main drawback for PDMS based strain sensors is their permeability, that hampers their performance in determined gas environments and it makes operation in-liquid immersion impossible due to unstable electrical measurements.

Materials such as SU-8 or polyimide (PI) are better candidates for in-liquid measurement stability while still being 1–2 orders of magnitude softer than standard MEMS materials. Polyimide-based strain gauges have been fabricated by evaporating metal on PI sheets for up to 2% tensile strain measurement at temperatures as high as 200 °C [8]. Similarly, metal strain sensors on SU-8 substrates have been reported to measure the forces exerted by small organisms such as *C. elegans* on top of microfabricated pillars [10].

In this paper, we present a force sensor based on SU-8 coated strain gauges for in-liquid measurements with a large bandwidth and a very high resolution, where some of the fabricated structures, measure forces as small as 10 pN.

2. Design

The chosen approach to achieve high sensitive in-liquid force sensing is based on the use of a hybrid stiffness microelectromechanical (MEM) device composed by thin and narrow SU-8 beams with metallic gauges embedded into them [14] placed in a Wheatstone bridge configuration as can be seen in Fig. 1a. The choice of metal as a strain sensor (as opposed to semi-conducting materials or polymer-based conducting materials) is motivated to have a low electronic noise, both Johnson, 1/f and shot noise. In particular we choose gold because

* Corresponding author.
E-mail address: cms@csem.ch (C. Martin-Olmos).

https://doi.org/10.1016/j.mee.2018.01.020
0167-9317/

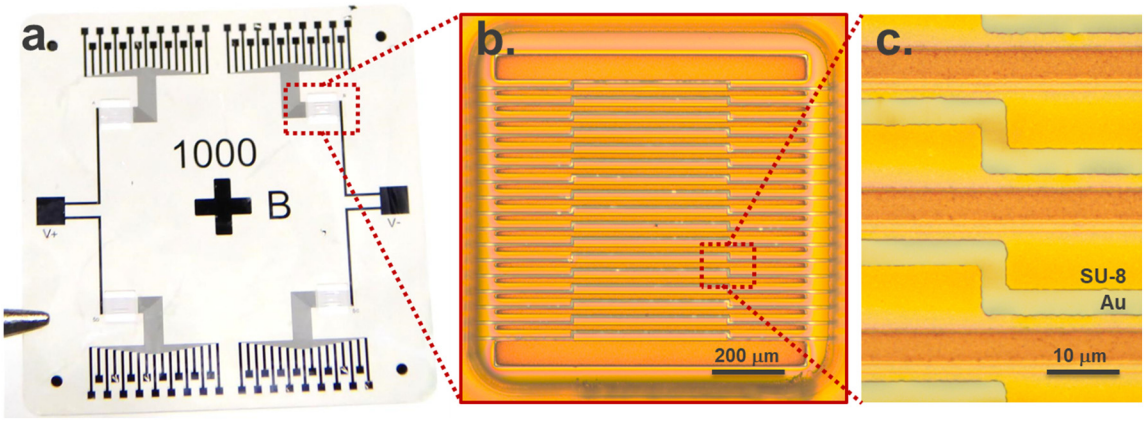

Fig. 1. Strain sensor device: a. A picture of the released device showing the four sets of strain sensors in a Wheatstone bridge configuration. b. An optical image of one of the sets of strain sensors when it was still attached to the Si wafer coated with a Cu layer. c. Zoom in of the U shape design of the strain gauges and their separation with the SU-8 coating and between gauges.

of its good resistivity and large Poison ratio, which also determines a large piezometallic coefficient. SU-8 has been selected not only because it can be patterned via optical lithography and its Young's modulus has an optimum value for the envisaged applications but also for its high dielectric strength and insulating capability even for very thin layers [19].

Initial finite element method (FEM) simulations estimate that devices that can be fabricated via standard UV lithography (lateral dimensions limited to 1 μm resolution), can yield minimum detectable values of force around ~500 $pN/\sqrt{Hz}$ over a large bandwidth due to the combination of metal gauges and AC bias (thus suppressing $1/f$ noise even more). Fig. 1b, taken with a 10× objective on an optical microscope, reveals gauges of 1 mm length with 3 μm width. There are three different gauge lengths: 600 μm, 850 μm and 1000 μm. These structures are meant to measure in-plane forces, therefore, to make them more sensitive the metal gauge has a U shape in the center shown with a zoom in Fig. 1c.

Within this first generation and regarding the width dimension of the gauges, we include devices with large safety margins to ensure good fabrication yield and devices for which we push the limits of our optical lithography equipment. After careful simulations using Finite Element Modelling we obtain a range for the responsivity of our devices ranging from 0.2 $\frac{ppm}{nN}$ ($L = 600$ μm, $w_{beam} = 20$ μm, $w_{res} = 4$ μm) till 0.6 $\frac{ppm}{nN}$ ($L = 850$ μm, $w_{beam} = 10$ μm, $w_{res} = 2$ μm). Considering a bias voltage of 1 V, and a noise of around 5 $\frac{nV}{\sqrt{Hz}}$ we can see that the estimated resolution is between 10 and 25 $\frac{pN}{\sqrt{Hz}}$.

3. Fabrication

The fabrication process of polymer coated strain sensors (shown in Fig. 1) is based on the multiple spin-coating, exposure and development of different thickness formulation of SU-8 resist (from Gersteltec) on a silicon wafer, being the latter used as a support.

The silicon wafer (100 mm diameter) is sputter-coated with 200 nm of copper (a 10 nm layer of Cr is also deposited to enhance adhesion) as shown in Fig. 2a. The first layer of SU-8 deposited is a thin formulation, GM1010 at 1500 rpm for a final thickness of 100 nm. The layer is soft baked (90 °C for 10 min) and exposed under UV light to pattern the

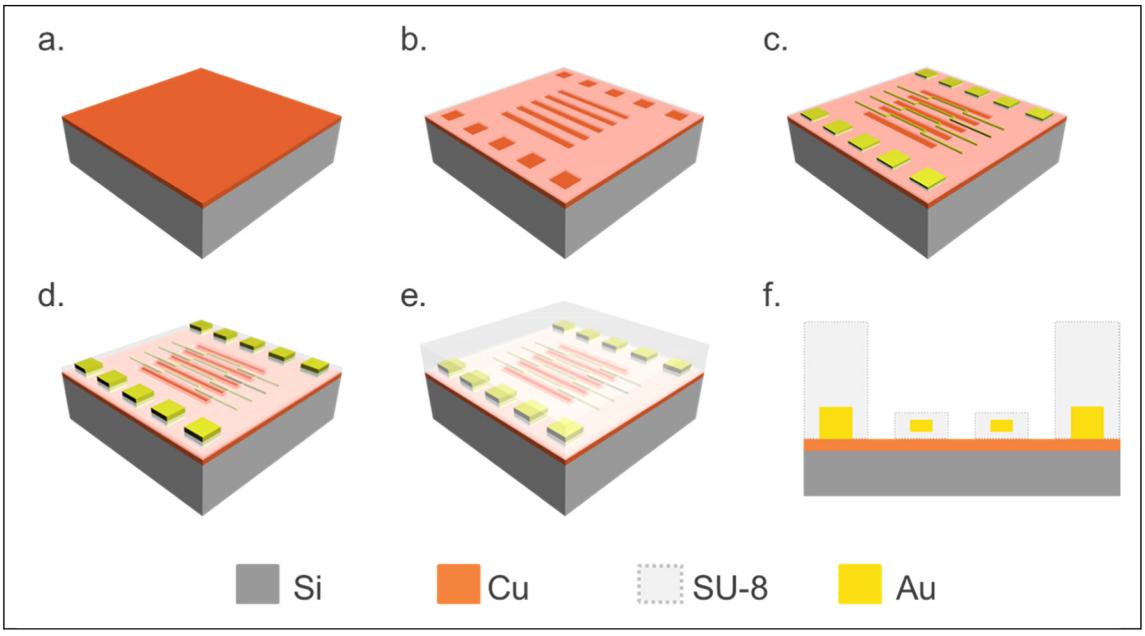

Fig. 2. Fabrication steps and device section: a. A silicon wafer is coated with Cu. b. A thin layer of SU-8 is deposited and fully processed. c. A gold evaporation is deposited through lift off process. d. A second thin layer is processed to fully coat the gold strain gauges. e. A thick layer of SU-8 is deposited and is fully processed to a final structure showed in cross section in f.

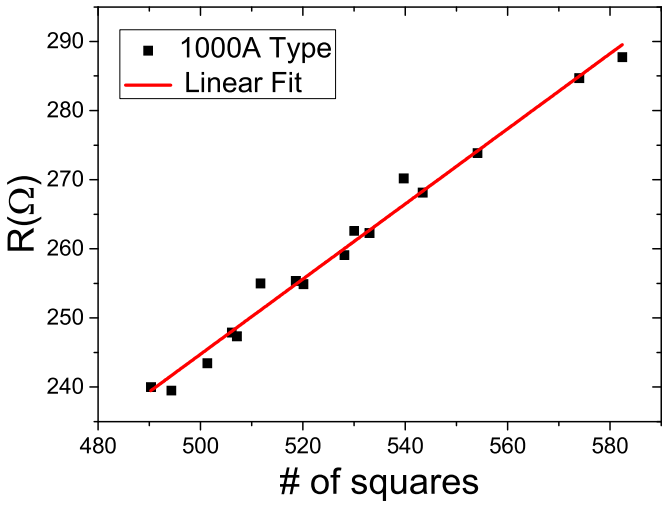

Fig. 3. Linear fit of an exemplary plot of R vs number of squares of the conductive path of a 1000 μm long strain sensor set. The deviation is rather small in all the measured cases.

Table 1
Experimental resistance in the fabricated strain sensors.

Strain gauge type	Measured resistance
600 μm length	1.0 ± 0.2 Ω/sq
850 μm length	0.6 ± 0.1 Ω/sq
1000 μm length	0.5 ± 0.1 Ω/sq

beams shape (140 mW/cm^2). Post exposure bake is performed at 90 °C for 10 min and the layer is developed immersing the wafer in propylene glycol monomethyl ether acetate (PGMEA) and rinsed with isopropanol (IPA) with the Fig. 2b appearance. A hard bake step is performed here following the parameters described in [20].

The wafer is now ready for deposition of a double resist layer for an optimized lift off process. First, we deposit and bake LOR resist and then a layer of 1 μm thick AZ1512 resist is deposited. The resist is exposed under UV light (60 mW/cm^2) for transferring the shape of the resistors and it is developed with AZ 726 MIF developer and deionized water.

Gold deposition is performed using an e-beam evaporator. A layer of Cr-Au-Cr is deposited in the ration of 5–60–5 nm. Cr is deposited to enhance the adhesion with the SU-8 layers (the inferior and superior). After e-beam deposition, lift off process is done using commercially available 1165 remover and IPA rinsing as exhibited in Fig. 2c. The wafer is then dehydrated again and ready for another thin layer of SU-8. This second layer of thin GM1010 SU-8 is identically deposited, exposed and soft and post exposure baked than the previous one (Fig. 2d). Nevertheless, this second time the thin SU-8 layer is not developed and instead a thick layer is deposited using GM1075 at 800 rpm for a final thickness of 450 μm. This layer is soft baked making a ramp from 60 °C to 90 °C during 30 min, remaining for 2 h at 90 °C and ramping down back to room temperature decreasing 2 °C per minute. The layer is exposed to UV light with 700 mW/cm^2. A post exposure bake is performed making a ramp from 60 °C to 90 °C with 1 °C per minute step, remaining for 45 min at 90 °C and ramping down back to room temperature at 2 °C per minute step (Fig. 2e).

Finally the wafer is fully developed by immersion in PGMEA and rinsed with IPA. A final hard bake process is done as detailed in [20]. Fig. 2f displays the cross section of the final device just before being released.

To release the chips from the silicon wafer, a Cu etching is performed with the commercially available ferric chloride based Cu etchant with an etch rate of 0.5 mil/min at 40 °C available at Sigma Aldrich. Once the copper is completely etched the chips are triple rinsed with DI water.

The overall stack of layers is transparent to keep compatibility with inverted optical microscopes as shown in Fig. 1a.

4. Results

4.1. Experimental resistance and comparison with simulation

The fabricated structures are measured with an AFM to precisely obtain the fabricated dimensions in terms of width and thickness of the SU-8 beam and the Au gauge. We observe a 20% increase of these final dimensions with the ones originally designed.

A manual probe station is used to obtain a current sweep from −500 μA to 500 μA at the two ends of each strain gauge with a step of 20 μA. These sweeps are fit to a line, as shown in Fig. 3, and we do this for at least 20 identical beams. Results are summarized in Table 1, and they show a relative dispersion of the resistance values of 10%. We believe this variation originates from the inherent precision of the optical lithography utilized to define the resistors. Since having very low variability of the resistance is paramount for a proper balancing of the resistive bridge, it is therefore important to address this in further generations of these devices.

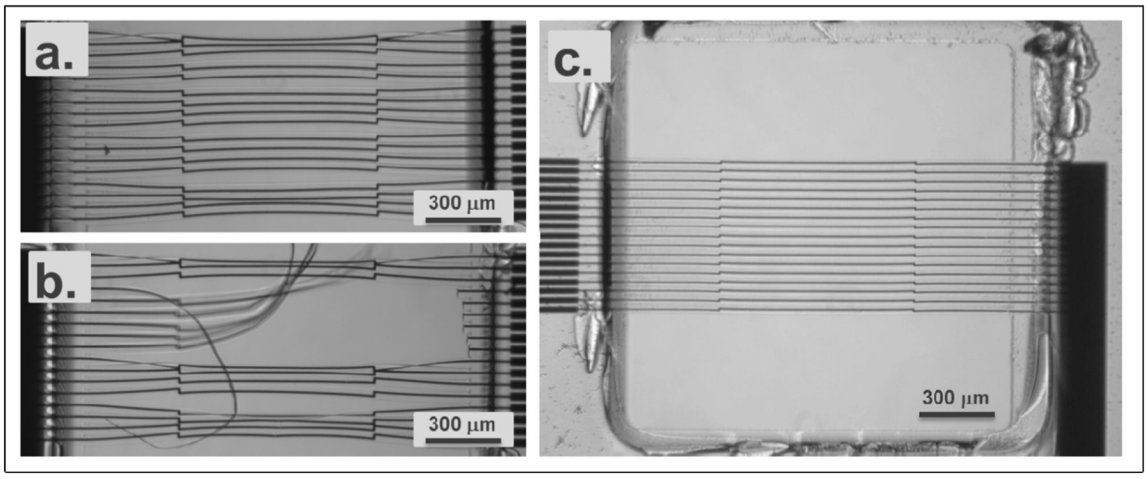

Fig. 4. Inverted microscope images of the sensing areas in the released devices. a. the capillary forces stuck a few strain sensors together. b. When drying the devices some strain sensors broke or detached. c. Intact sensing area after releasing the device.

4.2. Fabrication yield

Most of the structures are released without breaking or with any damage in the metal or polymer layer (Fig. 1a). Only a few devices present the Au metal discontinued in corners of the resistors and in the worst case, broken or twisted. In summary, a 80% yield is calculated when the released chips are remained in DI water until its use. Since these chips are made to be operated in liquid, they are stored in well plates filled with DI water.

When devices are dried with environmental evaporation (this might be necessary for example in order to characterize them with a probe station, as we present in the next paragraph) capillary forces provoke twists or stuck structures (Fig. 4a) in some cases and even, in the worst cases, broken beams (Fig. 4b). This step decreases the yield to a 50% of *arrays*, i.e. only half of the arrays have all the structures intact (Fig. 4c). If we count single beams, the yield is actually 70%. It is well known that this yield can be improved by means of a critical point dryer. In our case, this extra step is not necessary since the chips are aimed for an in-liquid use, thus drying is not part of the actual process.

5. Conclusion

Fabrication of high resolution force sensors with polymer coated metallic strain gauges that can be operated in liquid have been demonstrated. The strain sensors are well isolated by thin layers of SU-8 without experiencing cross-talk and, according to simulations, can detect forces as small as 10 pN. This enables a whole range of experiments that up to now were only accessible through very specific techniques.

Acknowledgements

This work is supported by Swiss National Science Foundation with the Ambizione career program CellStrates (PZ00P2_154900) and co-financed by CSEM. The authors are very grateful to Dr. Sebastian Jiguet for supplying the special thin layer formulations of SU-8. Also the authors want to thank the CMi-EPFL cleanroom facility and CSEM cleanroom facility and their respectively supporting staff members.

References

[1] J. Rajagopalan, M.T. Saif, MEMS sensors and microsystems for cell mechanobiology, J. Micromech. Microeng. 21 (5) (2011) 54002–54012.
[2] S. Hemanth, et al., Suspended microstructures of epoxy based photoresists fabricated with UV photolithography, Microelectron. Eng. 176 (Supplement C) (2017) 40–44.
[3] C. Liu, Recent developments in polymer MEMS, Adv. Mater. 19 (22) (2007) 3783–3790.
[4] M. Matschuk, H. Bruus, N.B. Larsen, Nanostructures for all-polymer microfluidic systems, Microelectron. Eng. 87 (5–8) (2010) 1379–1382.
[5] K.F. Lei, K.-F. Lee, M.-Y. Lee, Development of a flexible PDMS capacitive pressure sensor for plantar pressure measurement, Microelectron. Eng. 99 (2012) 1–5.
[6] E.L. Tan, et al., Implantable biosensors for real-time strain and pressure monitoring, Sensors (Basel) 8 (10) (2008) 6396–6406.
[7] S. Stassi, et al., Flexible tactile sensing based on piezoresistive composites: a review, Sensors (Basel) 14 (3) (2014) 5296–5332.
[8] D.J. Lichtenwalner, A.E. Hydrick, A.I. Kingon, Flexible thin film temperature and strain sensor array utilizing a novel sensing concept, Sensors Actuators A Phys. 135 (2) (2007) 593–597.
[9] J.L. Tan, et al., Cells lying on a bed of microneedles: an approach to isolate mechanical force, Proc. Natl. Acad. Sci. 100 (4) (2003) 1484–1489.
[10] J.C. Doll, et al., SU-8 force sensing pillar arrays for biological measurements, Lab Chip 9 (10) (2009) 1449–1454.
[11] G. Villanueva, et al., Piezoresistive cantilevers in a commercial CMOS technology for intermolecular force detection, Microelectron. Eng. 83 (4) (2006) 1302–1305.
[12] M. Moczała, et al., Fabrication and characterization of micromechanical bridges with strain sensors deposited using focused electron beam induced technology, Microelectron. Eng. 176 (Supplement C) (2017) 111–115.
[13] L.G. Villanueva, et al., Nonlinearity in nanomechanical cantilevers, Phys. Rev. B 87 (2) (2013).
[14] A. Johansson, et al., SU-8 cantilever chip interconnection, J. Micromech. Microeng. 16 (2) (2006) 314.
[15] M. Beygi, S. Mutlu, B. Güçlü, A microfabricated strain gauge array on polymer substrate for tactile neuroprostheses in rats, J. Micromech. Microeng. 26 (8) (2016).
[16] D.-W. Lee, Y.-S. Choi, A novel pressure sensor with a PDMS diaphragm, Microelectron. Eng. 85 (5–6) (2008) 1054–1058.
[17] T.H. da Costa, J.-W. Choi, A flexible two dimensional force sensor using PDMS nanocomposite, Microelectron. Eng. 174 (2017) 64–69.
[18] M.K. Filippidou, et al., A flexible strain sensor made of graphene nanoplatelets/polydimethylsiloxane nanocomposite, Microelectron. Eng. 142 (2015) 7–11.
[19] C. Martin-Olmos, et al., Conductivity of SU-8 thin films through atomic force microscopy nano-patterning, Adv. Funct. Mater. 22 (7) (2012) 1482–1488.
[20] C. Martin, et al., Stress and aging minimization in photoplastic AFM probes, Microelectron. Eng. 86 (4) (2009) 1226–1229.